

Synthetic Non-Parametric POD for Large Defects

Gert PERSSON, Håkan WIRDELIUS and Peter HAMMERSBERG

¹ Chalmers University of Technology, Gothenburg, Sweden
gert.persson@chalmers.se; hakan.wirdelius@chalmers.se; peter.hammersberg@chalmers.se

Abstract

Experimental POD results derived from an ultrasonic inspection procedure are validated by the use of the simulation software *simSUNDT*. Qualification of UT personnel within the Swedish nuclear industry has been conducted, according to the inspection procedure *UT-01*, since 1998. The *simSUNDT* software has in this paper been used in order to produce a multi parameter meta-model corresponding to the experimental set-up in *UT-01*. This has then been used in order to generate synthetic probability of detection by stochastic computation. For large defects the numerical POD shows the same interesting phenomena as can be seen in experimental setups with a high number of confident data where non-parametric estimation is used. Since the numerical model has no noise, and thus no assumptions about the statistical distribution of noise, it gives a unique possibility to study the deviation from Beren's type predicted POD based on distribution assumptions. The deterministic numerical signal response is studied in both time and frequency-plane, and this examination uncovers physical explanations to the POD behaviour for both fatigue and stress corrosion cracks.

Keywords: NDE simulation, simulated POD, stochastic, *simSUNDT*, *UT-01*

1. Introduction

Manufacturers are today experiencing an exceptional situation with higher demands on performance (lighter, more reliable and lower costs) and aggressive competition from all regions in the world. To be competitive on the global market, established manufacturers need to cut costs, reduce lead time to market and improve quality, simultaneously. Many industries still rely heavily on destructive testing techniques for identification of deviations such as defects and imperfections when producing components conforming to the quality requirements. Within the nuclear and aeronautic industry advanced forms of nondestructive testing methods (NDT) have been applied both for manufacturing control (e.g. welding) and in-service inspections since more than three decades. This development was driven by the introduction of structural design and risk based inspection programs developed from the damage tolerance concept.

New and stronger demands on reliability of used non-destructive methods and procedures (NDT/NDE) have enforced different strategies to quantify the inspection capability. The most dominant and frequently used method within the aero industry is the probability of detection (POD) methodology [1]. Traditionally POD curves are generated by thoroughly developed experimental procedures. The POD as a function of defect size is fitted to a large number of data points from experimental runs for each application where the testing technique is going to be used. The generation of POD curves is considered to be tedious, both time wise (the generation of at least 40 samples with controlled defect size is area of expertise in itself, with lead-times measured in quarters of a year rather than days) and economically. And yet is the possibility for studies of variability and robustness of the testing procedure limited; even parameter studies with verified simulation packages gets cumbersome with a growing number of control and noise factors with different variability constraints.

The European nuclear industry decided in the middle 1990's to develop an industry specific methodology in order to assess the NDT capacity, not only in detection but also as a tool of sizing and characterization. The ENIQ approach (European network of inspection

qualification) is characterised by what is known as the Technical Justification. This is a document that gathers evidence (experimental data, physical reasoning or by modelling) of the overall inspection system capacity, including equipment, procedure and a range of operators. This need of different approach of qualification is also justified by rigorous safety regulations, costs related to exclusive components and unplanned shut downs.

Traditionally all qualification methodologies have been empirically based with extensive experimental work with test blocks containing artificially produced defects of controlled size. An infinite number of variables and possibilities then have to be reduced into a limited group of statistically relevant NDT situations. Besides the problem of reconstructing the geometry and material of the real application, the fabricated defects also have to be introduced with a verified prescription of sizes and NDT characteristics. In the recent decade a number of mathematical models have been developed and used as tools within parts of these qualification processes. A thorough validated model has the ability to be an alternative or a complement to the experimental work in order to reduce the extensive cost that is associated with the previous procedures.

This study is based on the UT-01 procedure which specifies manual ultrasonic inspection of piping components within Swedish nuclear power plants [2]. The technical justification was developed according to the intentions of the ENIQ Recommended Practice 2 [3] and the procedure was qualified as such in 1997 (at SQC, the Swedish qualification centre). The first version of the UT-01 procedure comprised manual ultrasonic technique to detect, size and characterize fatigue and stress corrosion cracks. A large number of inspectors have been qualified according to this procedure and their results (i.e. in detection) have also been used in a study with the ambition to estimate subsequent POD curve [4].

A number of ongoing projects [5,6] address the possibility to enable simulated data to be used within the development of POD curves. This paper is part of a project that intends to develop a slightly different methodology. An optimized experimental phase with representative samples, but easy to manufacture, is combined with much more efficiently retrieved simulated data. In this case a computational fast simulator was generated by fitting a multi-parameter prediction model to the simulation software simSUNDT. POD curves of the probability of detection as function of defect size at different defect depths were then produced by Monte Carlo simulation introducing variations in the control factors with a physical interpretation in the emulator.

The suggested approach to generate synthetic POD curves is to use meta-models of experimentally validated mathematical model of well defined NDT procedure. These meta-models can then also be used in e.g. some full factorial investigations of different correlations between various NDT parameters with integrity or/and production process and quality variables. The NDT information can thereby not only be used for component lifetime estimations but also contribute to deeper understanding of process variations.

2. Ultrasonic simulation software

There do exist a limited amount of models that cover the whole ultrasonic testing procedure, that include the modeling of transmitting and receiving probes, the scattering by defects and the calibration. In order to handle this rather complex modeling task different kind of presumptions and approximations have rendered in different simulation software, each defined by their individual possibilities and range of validity. Chapman [7] employs geometrical theory of diffraction for some simple crack shapes and Fellingner et al [8] have developed a type of finite integration technique (EFIT) essentially for a two-dimensional treatment of various types of defects. Lhémy et al [9] employs Kirchhoff's diffraction theory that enables their model to handle more complex geometries in 3D (CIVA).

2.1 simSUNDT software

The simSUNDT program [10] is a Windows®-based preprocessor and postprocessor together with a mathematical kernel (UTDefect, [11-15]) dealing with the actual mathematical modeling. The UTDefect computer code has been developed at the Dept. of Mechanics at Chalmers University of Technology and has been experimentally validated and verified [13-15]. The model employs various integral transforms and integral equation techniques to model probes and the scattering by defects. The software simulates the whole testing procedure with the contact probes (of arbitrary type, angle and size) acting in pulse-echo or tandem inspection situations.

The model is completely three dimensional though the component is two dimensional (infinite plate with finite or infinite thickness) bounded by the scanning surface where one or two probes are scanning the object within a rectangular mesh. The probe is modeled by an assumed effective area beneath the probe, used as boundary conditions in a half-space elastodynamic wave propagation problem. This enables an adaptation to a variety of realistic parameters related to the probe, e.g. wave type, angle, crystal (i.e. size and shape), focus depth and contact conditions. In addition to the option of specifying the contact conditions it is also possible to suppress the "wrong" wave component, which enhance the possibility to make an interpretation of the received signal. The receiver is modeled by applying a reciprocity argument by Auld [16].

In order to completely simulate the actual NDT situation, an option of calibration against a reference reflector is included in the software. The calibration procedure with a side-drilled hole is treated exactly, with the use of the cylindrical cavity, while the flat-bottom hole is approximated with an open circular crack.

2.2 Experimental validation of the simSUNDT software

An ultrasonic benchmark study was initiated by the World Federation of NDE Centers and practically conducted by Commissariat à l'énergie atomique (CEA, France) during the year of 2009 [17]. The experiments included experimentally measured signal responses of side-drilled holes, flat-bottom holes and rectangular surface breaking defects (slots). The main interest was to make experimental data available in order to validate the capability of different mathematical models of ultrasonic NDT techniques.

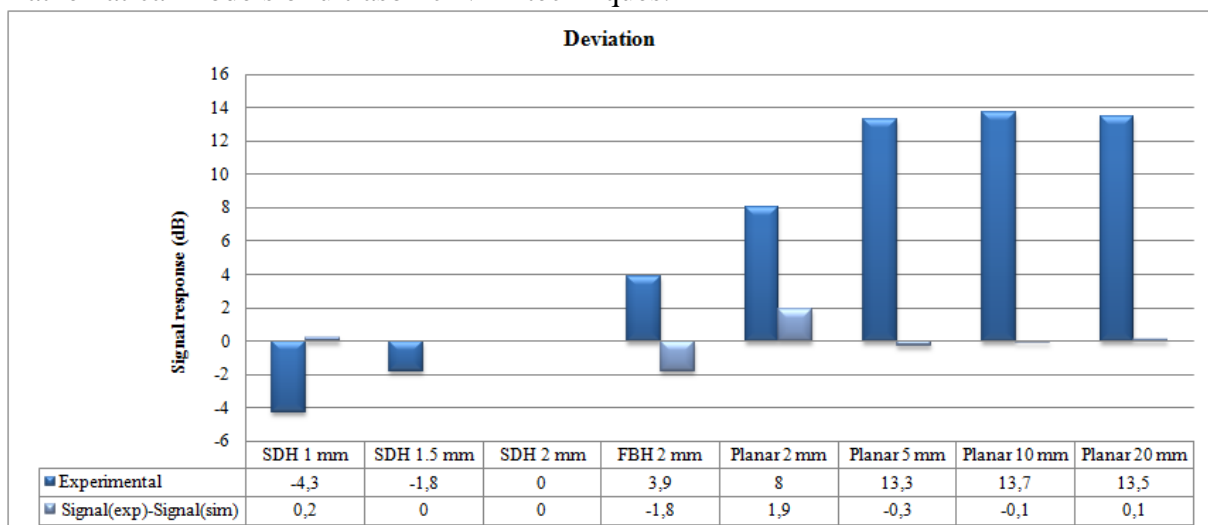


Figure 1. Deviation between calibrated (SDH 2 mm) experimental signal responses and corresponding simulated situations.

The test specimen was manufactured in stainless steel (density 7950kg/m^3 , P-wave speed 5748m/s and S-wave speed 3157m/s) with 12 different artificial defects. The surface breaking defects were slots (width of 0.3 mm) in two different lengths (5 and 40 mm) and in four different heights ($2, 5, 10$ and 20 mm). The flat-bottom hole (3 mm in diameter) was tilted 45 degrees in order to achieve specular reflection using a 45 degree UT probe. Three side-drilled holes ($1, 1.5$ and 2mm in diameter) were machined into the test piece with the largest used as reference defect.

The benchmark included two conventional 45 degree shear wave transducers with different crystals and one phased array probe that previously have been validated with the *simSUNDT* software [15]. Both conventional probes (WB45 and MSWQC45) could be used within the *UT-01* procedure but as can be deduced in figure 1 the agreement found, between simulations and experiment, was very good for the circular contact probe and this was therefore our choice. The diameter of the crystal was specified as 6.35 mm and the centre frequency 2.25 MHz (44% in bandwidth). It should be noted that a two dimensional defect (surface breaking strip-like crack) was used in the simulations which gives very good agreement with corresponding slot of 40 mm in length (see figure 1). The signal response from the 5 mm slot was typically $2\text{-}4\text{ dB}$ below corresponding 40 mm slot.

3. Parametric POD according to the *UT-01* Procedure

The *UT-01* procedure specifies manual ultrasonic inspection of piping components within Swedish nuclear power plants and cover techniques for detection, sizing and characterization. It covers both fatigue cracks and intergranular stress corrosion cracks (IGSCC). The procedure specifies in details parameters such as; components, defects, level of competence (personnel), method, equipment, calibration and inspection procedure with e.g. detection criteria, characterization procedure and techniques for sizing of defects.

All identifiable parameters in the procedure, for a pulse-echo situation according to fig.2, are subdivided into influential and essential parameters. Influential parameters are factors that can potentially influence the outcome of an inspection and essential parameters are those parameters whose change in value would actually affect a particular inspection so that it no longer meets its defined objectives.

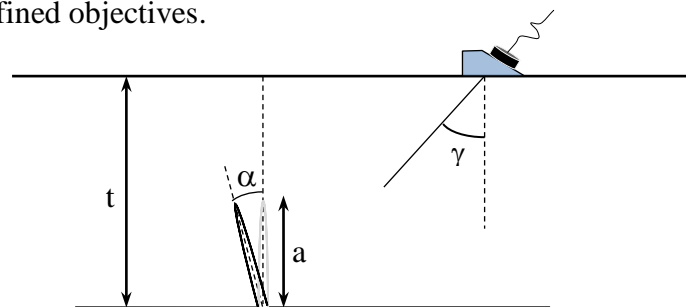


Figure 2. The geometry of the surface breaking crack in a pulse-echo situation

The latter have to be addressed with a subdivision into Set 1 and Set 2 parameters. Essential parameters that are identified as Set 1 must be specified with correlating uncertainties and their distribution. Based on the *UT-01* documentation [2], the corresponding *Technical Justification* [18] and restraining to parameters that are available within the *simSUNDT* software the identified essential parameters are defined in table 1 and 2.

In this study the defect size/width a is treated as a Set 2 parameter since it is a control factor. It was identified that the wall thickness did not seem to be a significant parameter in itself

since the applied calibration, distance amplitude correction (DAC), intends to withdraw this as an essential parameter.

In order to quantify the capability of the *UT-01* procedure, data recorded during 9 years of qualification was composed in a project [4]. Results from investigation of 97 cracks from 55 different test cases involving 41 different ultrasonic technicians (level II according to EN 473) were used for the estimation of the POD curves for this specific procedure. For the Binomial distribution the so-called probit and logit links were used.

When only stress corrosion cracks (IGSCC) were considered, the POD was estimated in the report [4] as;

$$POD = \Phi(0.1218 + 0.3720 \cdot \ln(a)) \quad (1)$$

where Φ denotes the normalised Gaussian distribution.

And when only the fatigue cracks were considered the estimated POD function was estimated as;

$$POD = \Phi(0.6503 + 0.3720 \cdot \ln(a)) \quad (2)$$

showing a significant higher detection rate for fatigue cracks than IGSCC. Both curves can be found in figure 3.

4. Simulation of non-parametric POD

The methodology developed and described in [19] is here used to emulate non-parametric POD curves. The ultrasonic simulation software *simSUNDT* is used as kernel for stochastic computations in the sense that a meta-model is built on deterministic computations made by *simSUNDT*. Using a central composite designs method (essentially cubic face centred) a total of 1000 simulations were executed with *simSUNDT*. The response surface for the normalised DAC signal response was created by surface fitting of Hardy's MultiQuadratics radial basis functions to the simulated values. The stochastic simulation was made by using a Latin hypercube sampling (LHS) for creation of 5000 random designs for each data set, data according to table 1.

Table 1. Distributions of Set 1 parameters

Stochastic distributed parameters	Distribution	Mean	Delta	SD
Probe angle (γ)	Normal	45		0.8
Probe diameter (γ)	Normal	6.6		0.32
Defect tilt angle (α)	Uniform		15	
Defect skew angle	Uniform		20	
Defect tilt angle (α)	Normal dist.1	0		15
Defect skew angle	Normal dist.1	0		20
Defect tilt angle (α)	Normal dist.2	0		7.5
Defect skew angle	Normal dist.2	0		10

The POD for the stochastic computation is measured as the percentage of the 5000 simulated signal responses above -6 dB. The different POD curves in the figure 3 represent different distribution of tilt and skew angles according to table 1, compared to experimentally estimated parametric POD for fatigue cracks and IGSCC using equation (1) and (2). The comparisons show that

- A small fatigue crack is quite well modelled by a crack having a normal distribution, with a mean of 0° with two standard deviations of both skew and tilt (see table 1).
- A small IGSCC is relatively well described by a more uniform distribution of skew and tilt angle, i.e. no preferred growth direction within the specified limits (see table 1).

The technique of building a meta-model (response surface) for the stochastic simulation starts with identifying the essential parameters. As in the experimental POD study [8] the object thickness is reduced as an essential parameter by the calibration procedure within *UT-01*. The defect size (a) is used as a control factor and the Set 2 parameters are treated as constants. The benchmark [17] included the conventional circular 2.25 MHz 45° shear wave contact transducer MSWQC45, which is a possible choice within the *UT-01* procedure in the investigation [4]. Probe parameters are found in Table 2, and the probe are modelled with a cosine square spectrum.

For large defects we see that the simulated POD, in figure 3, is actually decreasing, whereas the probit curves fitted to the experimental data do not. Comparing the experimentally determined POD and the simulations for a 2.25MHz probe, we see that the normal dist.1 follows the experimental fatigue crack very well up to 10 mm. For larger cracks the simulated POD yields a decreased signal response.

Here we should note that the material we are referring to, i.e. the *UT-01* investigation [4], contains few large cracks since the investigation were focused on qualification defects that is in the lower range of the POD curve. The experimentally determined Gaussian distributed POD-curves from the procedure *UT-01* is constructed from 14 and 83 different defects for the IGSCC and the fatigue crack, respectively. For the data used to construct the IGSCC-POD there were 12 cracks less than 8 mm and the 95% confidence bands are both of the order 10%. Most of these surface-breaking cracks can probably then not be considered as “large” cracks. For experiments, with a small amount of data points given, it is common to use a parametric model hypothesis (with a given law), like Berens parametric model hypothesis [20], to represent the POD. The general POD behaviour is then always mastered, giving the POD the general shape rising from 0% to 100%, with the parameters adjusted to best fit the given data. The hypothesis, however, includes some assumptions not always correct, such as that a normally distributed signal response. It is shown in [21] that this is not the case for simulated defects, due to the curved transfer function, and probably not for real defects Which would probably also be the case for real defects in an experimental study.

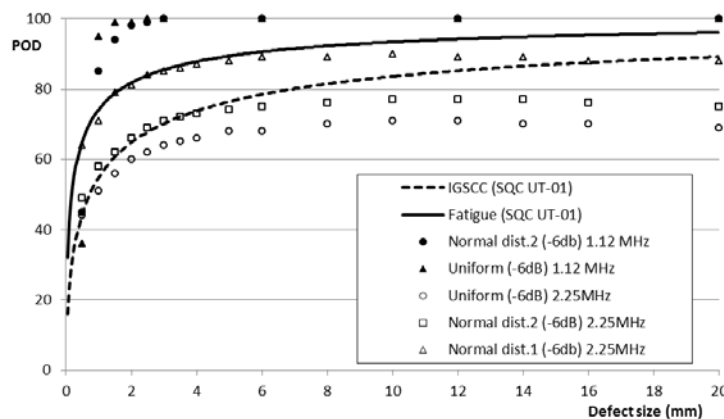


Figure 3. Experimentally estimated parametric POD (Eqs. (1) and (2)) compared with simulated POD

In experimentally derived POD curves, where a high number of noisy observations are used for a non-parametric estimation of the POD, methods like quantile regression and kernel smoothing yields a smooth response curve. Here it is sometimes noted that for large enough defects there is a drop in the empirical POD.

This behaviour, found in empirical POD and in models where no distribution is presumed, seems to be exposed by the simulations for the 2.25 MHz probe in figure 3. To validate the expected behaviour of the simulated response there is a need to keep the full spectra of the underlying data for Eq.(1)(2), since a comparison to the Gaussian distributed computations is misleading.

For the 1.12 MHz probe there is no drop in the simulated POD for large defects, the simulated POD reaches 100% for both distributions. The comparison between the 2.25 MHz and the 1.12 MHz probe indicates that the differences in behaviour is a phenomena due to resonances.

Table 2. The Set 2 parameters

Probe parameter			Defect parameter	
Center frequency	2.25 MHz	1.12 MHz	Defect width (a)	10 and 20 mm
Bandwidth	0.99 MHz	0.50 MHz	Defect tilt angle (α)	-10° , 0° and 10°
Probe diameter	6.5 mm		Defect skew angle	0°
Probe angle (γ)	45°		Defect depth (reduced due to DAC)	35 mm
Couplant	0.4		Wave speed (C_L)	5720 m/s
Density	7950 kg/m ³		Wave speed (C_S)	3120 m/s

To investigate this resonance phenomena further, time signals needs to be studied.

Using the *simSUNDT* software a surface breaking crack, specified testing situation according to table 2, is investigated for nominal values. The deterministic computed crack response in figure 4 corresponds to the simulated cracks, of width 10 mm, in the stochastic computations. Signal response can be found in table 3. When making the time-of-flight computations, used to identify the different contributions, it has been assumed that the wave speed of the Rayleigh waves is 93% of C_S .

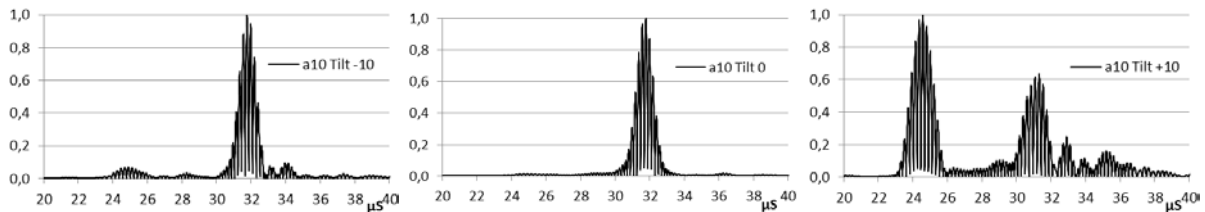


Figure 4 a, b, c. Normalized time signal response of cracks of width 10 mm according to table 2, tilt -10° , 0° and $+10^\circ$ respectively

Figure 4b shows the response of the untilted surface breaking crack. The response is dominated by the signal reflected in the back surface of the sample, corresponding to an s-wave reflected as an s-wave.

Table 3. Maximum signal response

Figure	4a	4b	4c	5a	5b	5c	6a	6b	6c
Defect width (a)	10	10	10	20	20	20	20	20	20
Defect tilt angle (α)	-10°	0°	10°	-10°	0°	10°	-10°	0°	10°
Defect skew angle	0°	0°	0°	0°	0°	0°	20°	20°	20°
Respons (dB)	11	19	10	12	19	12	-23	-16	-21

Figure 4a shows the crack with a positive 10° tilt. The dominating reflected response remains at approx 32 μ s and we can see two smaller diffracted responses at 25 and 28 μ s. The first contains of s-waves that, after interacting with the crack, travelled over the crack surface as Rayleigh waves and then diffracted from both the crack tip and the back surface as p-waves.

Furthermore there is a diffracted signal at 34 μs that could be explained by s-waves hitting the back surface, travelling over the crack surface three times, and finally diffracting as p-waves from the crack tip.

Figure 4c, however, shows a somewhat different behaviour. The first diffracted field is now dominating the signal response and the two later diffracted fields have also grown in terms of signal response. Due to the mode conversions the main energy have travelled from the reflected to the diffracted response. The energy is transported by the non-dissipative Rayleigh surface waves.

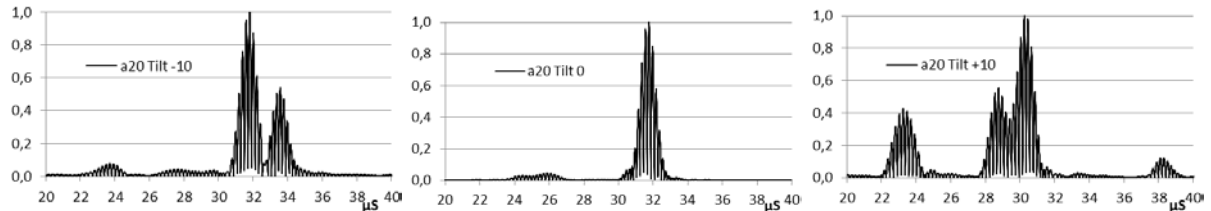


Figure 5 a, b, c. Normalized time signal response of cracks of width 20 mm according to table 2, tilt -10° , 0° and $+10^\circ$ respectively

For the 20 mm crack in figure 5 we see that both the negative (5a) and positive (5c) 10° tilted crack shows a behaviour where energy is transported from the reflected to the diffracted field due to mode conversions.

In a corresponding manner we can study the effect of a 20° skew combined with a 10° tilt, for a crack of width 20 mm, in figure 6. It is clear that both skew and tilt have a large influence on the conversion of wave modes of the reflected energy. It is also important to note that the DAC-calibration still is made for an SDH with 0° skew.

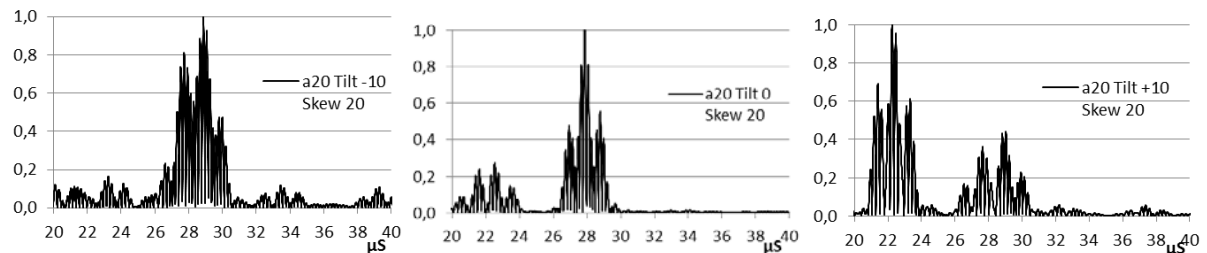


Figure 6 a, b, c. Normalized time signal response of cracks of width 20 mm according to table2, skew 20° and tilt -10° , 0° and $+10^\circ$ respectively

Furthermore, the significant change of signal response in figure 3 when the central frequency of the probe is changed from 2.25 MHz to 1.12 MHz is somewhat surprising. The 1.12 MHz probe shows a behaviour where it asymptotically yields a POD of 100%. This is unexpected since earlier investigations [22] have shown that changes in the frequency gives small changes in the signal response. However, this was made for a phased array probe and the variations of the frequency in that study might not be valid for the actual meta-model of a single-probe testing situation. Furthermore, the Set 1 and Set 2 parameters introduced in the *UT-01* procedure, stated that the central frequency was a less influencing Set 2 parameter.

The present computation shows that, before further investigations are made concerning the statistical distributions of the Set 1 parameters, the Set 2 parameters needs to be explored using fractional design of experiments for screening.

If we decrease the probe frequency with a factor two, the wavelength is increased by a factor two and we would expect a smaller response from small defects since the relative size of the defect gets smaller compared to the wavelength i.e. it should be more difficult to detect the small defects. The numerical results, on the other hand, shows the opposite. This is due to the fact that a lower frequency gives a wider ultrasonic beam from the probe, that is we get a higher level of detection of angled defects. This is a well-known phenomena in practical

testing situations. We can also note that the difference in POD, between cracks with uniform and normal-distributed defect angles, decreases for the 1.12 MHz probe.

In a further investigation of the deterministic response of the *simSUNDT* computations we study the signal response for the nominal values, according to table 2, for the 2.25 MHz probe. Figure 7 shows the signal response for various tilt angle, crack width and probe frequency, with all cracks having the skew angle of 0° . It seems like, in an overall sense, that the signal response decreases for larger cracks when the angling of the defect increases. The variation of the individual responses, as a function of crack width, can be interpreted in term of resonances. We can conclude that in a stochastic computation, were a defect is specified a certain angled distribution, the signal response will be lower than for the nominal deterministic value, thus giving a lower POD for large cracks.

The reasoning above is of course only valid for this specific 2.25 MHz probe, as indicated by the 1.12 MHz probe in figure 3, using a probe with a different central frequency would give another response.

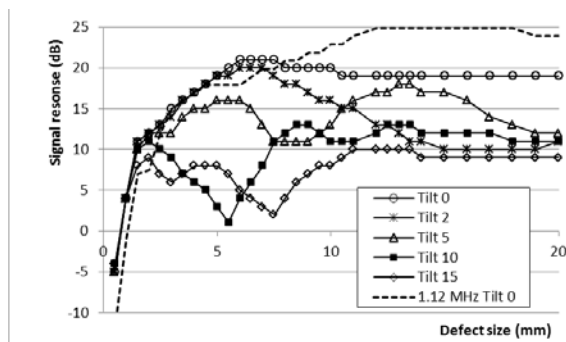


Figure 7. Normalized signal response vs crack width for different tilt angles and central frequency.

Making a similar comparison in figure 7 for the 1.12 and 2.25 MHz probe, untilted cracks, shows that the 1.12 MHz probe yields a higher response for larger cracks than the 2.25 MHz probe. Conclusion is that this indicates a higher POD for a corresponding stochastic computation, which is also seen in fig.3.

It should also be recalled that for the probe with half the original frequency we get a larger smallest detectable defect size. This follows the wavelength reasoning above and is also indicated in figure 7 where the envelope of the 1.12 MHz detection curves is much steeper than the corresponding for 2.25 MHz. This might be of interest in a future investigation of signal response for small defects.

5. Conclusions

Stochastic computation of simulated POD by the use of a meta-model based on *simSUNDT* shows that for fatigue cracks the reflection is dominating the signal response and SCC is dominated by diffraction. Deterministic computations further support this claim.

The, sometimes noted, drop in empirical POD for large enough defects is explained in terms of resonances for both fatigue and stress-corrosion cracks. Comparison is made with experimental data.

To validate the expected behaviour of the simulated response there is a need of the underlying data for the parametric probit-curves, since a comparison with the non-parametric simulations is misleading.

References

1. "Nondestructive Evaluation System Reliability Assessment", MIL-HDBK-1823A (2009).

2. C. Ericson, "Provningsprocedur för manuell ultraljudsprovning av rör och komponenter", UT-01 rev2, Swedish Nuclear Power Plant Owners, (2010).
3. ENIQ Recommended Practice 2: "Recommended Contents for a Technical" Justification, <http://safelife.jrc.ec.europa.eu/eniq/publications/complete.php>
4. T. Jelinek, L. Tidström and B. Brickstad, "Probability of Detection for the Ultrasonic Technique according to the UT-01 Procedure", SKI Report 2005:03, Stockholm (2005).
5. Model Assisted POD working group, <http://www.cnde.iastate.edu/MAPOD>
6. F. Jensen, S. Mahaut, P. Calmon and C. Poidevin, "Simulation based POD evaluation of NDI techniques", 10th European conference on non-destructive testing, Moscow (2010).
7. R.K. Chapman, "A System Model for the Ultrasonic Inspection of Smooth Planar Cracks", J. Nondestr. Eval. 9, 197-211 (1990).
8. P. Fellinger, R. Marklein, K.J. Langenberg and S. Klaholz, "Numerical Modelling of Elastic Wave Propagation and Scattering with EFIT-Elastodynamic Finite Integration Technique, Wave Motion 21, pp. 47-66 (1995).
9. A. Lhémy, P. Calmon, I. Levær-Taïbi, R. Raillon and L. Paradis, "Modeling Tools for Ultrasonic Inspection of Welds", NDT & E International 33, pp. 499-513 (2000).
10. G. Persson and H. Wirdelius, "Recent survey and application of the simSUNDT software", QNDE 2009, AIP Conference Proceedings, 1211 s. 2125-2132 (2009).
11. A. Boström and H. Wirdelius, "Ultrasonic probe modeling and non-destructive crack detection", J. Acoust. Soc. Am. 97, pp. 2836-2848 (1995).
12. P. Bøvik and A. Boström, "A model of ultrasonic non-destructive testing for internal and subsurface cracks", J. Acoust. Soc. Am. 102, pp. 2723-2733 (1997).
13. A. Boström and P.-Å. Jansson, Developments of UTDefect: rough cracks and probe arrays, SKI report 97:28, Swedish Nuclear Power Inspectorate (1997).
14. A.S. Eriksson, A. Boström and H. Wirdelius, SKI Report 97:1, Swedish Nuclear Power Inspectorate (1997).
15. H. Wirdelius, "Experimental validation of the UTDefect simulation software", Proc. 6th Int. Conf. on NDE in Relation to Structural Integrity for Nuclear and Pressurized Components, Budapest (2007).
16. B.A. Auld, "General Electromechanical Reciprocity Relations Applied to the Calculation of Elastic Wave Scattering", Wave Motion, vol. 1, pp. 3-10 (1979).
17. L. Schmerr, 2009 Ultrasonic benchmarks Part II – problems, (<http://www.wfndec.org>)
18. M. Strand, "Teknisk motivering Projekt UT01", ÅF Report 505179-RAPP-01, (2010).
19. H. Wirdelius and G. Persson, "Simulation Based Validation of the Detection Capacity of an Ultrasonic Inspection Procedure", International Journal of Fatigue (In press)
20. A.P. Berens. "NDE Reliability Data Analysis." ASM Metals Handbook, Volume 17, 9th Edition: Nondestructive Evaluation and Quality Control. ASM International, Materials Park, Ohio (1988).
21. G. Persson, P Hammersberg and H. Wirdelius, "POD generated by monte carlo simulation using a meta-model based on the simSUNDT software", QNDE 2011, AIP Conference Proceedings, ISBN 978-0-7354-1013-8 (2011).
22. P Hammersberg, G. Persson, and H. Wirdelius, "Emulation of POD curves from synthetic data of phased array ultrasound testing", QNDE 2011, AIP Conference Proceedings, ISBN 978-0-7354-1013-8 (2011).